Unexpected central-memory CD8+ T cell reduction hampers the antitumor efficacy of mogamulizumab (anti-CC chemokine receptor 4 mAb) treatment

Yuka Maeda
National Cancer Centre
Hisashi Wada (hwada@gesurg.med.osaka-u.ac.jp)
Osaka University Graduate School of Medicine
Takuro Saito
Osaka University Graduate School of Medicine
Daisuke Sugiyama
Nagoya University
Takuma Irie
National Cancer Centre
Kodai Minoura
Naogya University Graduate School of Medicine https://orcid.org/0000-0003-3221-329X
Susumu Suzuki
Aichi Medical University School of Medicine
Takashi Kojima
National Cancer Center Hospital East
Kazuhiro Kakimi
University of Tokyo Hospital
Jun Nakajima
University of Tokyo
Takeru Funakoshi
Keio University School of Medicine
Shinsuke Iida
Nagoya City University Graduate School of Medical Sciences
Mikio Oka
Kawasaki Medical School
Teppei Shimamura
Nagoya University Graduate School of Medicine
Toshihiko Doi
National Cancer Center
Yuichiro Doki
Osaka University

Eiichi Nakayama
Kawasaki University of Medical Welfare,
Ryuzo Ueda (uedaryu@aichi-med-u.ac.jp)
Aichi Medical University
Hiroyoshi Nishikawa (hnishika@ncc.go.jp)
National Cancer Centre https://orcid.org/0000-0001-6563-9807

Article

Keywords: CD8+ T cell reduction, antitumor efficacy, mogamulizumab treatment, cancer immunotherapy, Treg cell-targeted therapies

Posted Date: September 15th, 2020

DOI: https://doi.org/10.21203/rs.3.rs-73503/v1

Abstract

Developing Treg cell-targeted therapies is an important aspect in cancer immunotherapy. Here, we investigate anti-CCR4 mAb (mogamulizumab) with solid cancer patients in phase 1b clinical trial based on the predominant detection of CCR4-expressing eTreg cells in tumors. While eTreg cells in peripheral blood were significantly decreased after mogamulizumab administration in all patients, clinical responses were hardly detected. Comprehensive immune-monitoring revealed that concomitant reduction of central-memory $CD8^+$ T cells with CCR4 expression, that reportedly play an important role in antitumor activity. This reduction was subsided in long survivors in whom central-memory $CD8^+$ T cells possessed lower CCR4 expression and/or NK cells exhibited an exhausted phenotype. Thus, excess doses of mogamulizumab harboring enhanced antibody-dependent cellular cytotoxicity could unexpectedly deplete central-memory $CD8^+$ T cells with CCR4 expression. We therefore need to carefully determine the optimal dose of mogamulizumab for successful clinical application as cancer immunotherapy to avoid unexpected depletion of effector components.

Introduction

Genetic instability is an evolving hallmark of cancer cells; consequently, cancer cells frequently possess gene alterations that generate abnormal proteins [1]. These abnormal proteins are recognized as non-self antigens (termed neoantigens) by the immune system and antitumor immune responses are elicited (cancer immunosurveillance) [2, 3]. Therefore, clinically apparent cancer compels two crucial processes during the development; 1) the reduction of immunogenicity by decreasing the expression of abnormal proteins that can readily induce immune responses, and 2) the establishment of immune escape mechanisms involved in multiple immune suppressive machineries such as those involving immunosuppressive cells and immunosuppressive molecules [4]. Cancer immunotherapy represented by immune checkpoint blockade (ICB) unleashes the effects of effector T cells and kills cancer cells, resulting in tumor regression across multiple cancer types [5]. Yet, more than half of treated patients fail to respond to ICB, even in combination therapies; therefore, developing more effective therapies is definitely required [6].

Regulatory T (Treg) cells expressing the transcription factor forkhead box P3 (FoxP3) are an immunosuppressive $CD4^+$ T cell subset and are indispensable for the maintenance of self-tolerance and immune homeostasis [7, 8, 9] . In addition to immune checkpoint molecules, Treg cells hinder protective cancer immunosurveillance in healthy individuals and hamper effective antitumor immune responses in tumor-bearing hosts. Accordingly, high frequency of Treg cells and their dominance to effector T cells in the tumor microenvironment (TME) are associated with poor prognosis in various types of cancer [10, 11, 12, 13]. Hence, Treg cells are an attractive therapeutic target for cancer immunotherapy. It has been shown that selective depletion of Treg cells robustly augments antitumor immune responses and contributes to tumor eradication in animal models [13, 14, 15]. In humans, previous studies have examined the effects of Treg cell depletion by targeting CD25 with antibodies or a recombinant protein composed of IL-2 and the active domain of the diphtheria toxin, since Treg cells were originally identified as $CD25^+CD4^+$ T cells [7]. However,

anti-CD25 mAb depletes both effector T cells and Treg cells; consequently, neither antitumor T cell responses nor antibody production is observed [13, 14, 15, 16, 17]. As CD25 expression is induced upon the activation of effector T cells, CD25-targeted Treg-cell depletion may be accompanied by a reduction in effector T cells [18]. In addition, cyclophosphamide treatment, which reportedly depletes Treg cells in mouse models, combined with peptide vaccination successfully achieved Treg cell depletion, leading to a promising clinical impact in breast cancer patients [19]. However, this combination study failed to show clinical effectiveness in a phase III study, implying the importance of more selective depletion methods [20]. Moreover, given the crucial role of Treg cells in self-tolerance, Treg cell depletion on the whole can trigger autoimmunity in animal models [8, 15, 21]. An important issue is therefore how Treg cells can be controlled to evoke and augment antitumor immunity without inducing deleterious autoimmunity, strongly indicating the necessity of developing Treg cell depletion methods with superior selectivity to eliminate tumor-infiltrating Treg cells.

To identify the molecules specifically targeting tumor-infiltrating Treg cells, the accurate identification of Treg cells is essential, although FoxP3$^+$ T cells in humans are heterogeneous in phenotype and function due to the upregulation of FoxP3 in naive T cells upon T-cell receptor (TCR) stimulation [9, 13, 22]. Accordingly, human FoxP3$^+$CD4$^+$ T cells are fractionated into the following three subsets based on the expression levels of the naive T cell marker CD45RA and FoxP3 or CD25: Fraction (Fr.) I naive Treg cells (CD45RA$^+$CD25^{low}FoxP3^{low}CD4$^+$); Fr. II effector Treg (eTreg) cells (CD45RA$^-$CD25^{high}FoxP3^{high}CD4$^+$); and Fr. III non-Treg cells (CD45RA$^-$CD25^{low}FoxP3^{low}CD4$^+$). Fr. II eTreg cells, which possess high CTLA-4 expression and strong immune suppressive activity, are the predominant tumor-infiltrating FoxP3$^+$CD4$^+$ T cells found in the majority of cancers [9, 13, 22]. We have shown that C-C chemokine receptor (CCR) 4 is highly expressed by eTreg cells, probably through the involvement of C-C motif chemokine 22 (CCL22) for the infiltration of Treg cells into the TME, and that Treg cell depletion via targeting of CCR4 induces increased tumor antigen-specific CD4$^+$ and CD8$^+$ T cell responses [13, 23].

A phase 1a clinical trial of Treg cell depletion by administration of anti-CCR4 mAb (mogamulizumab, KW-0761) for advanced or recurrent solid tumor patients revealed a significant reduction of eTreg cells in the peripheral blood [24]. While humoral responses against NY-ESO-1 and XAGE1 antigens were observed in patients with NY-ESO-1 and XAGE1-expressing tumors, respectively, clinical responses were unfortunately not observed in most patients [24]. Here, we examined patient samples enrolled in a Phase 1b clinical trial with mogamulizumab monotherapy via addressing comprehensive immunological changes pre- and post-mogamulizumab administration with multicolor flow cytometry and CyTOF. We found an unexpected reduction of central-memory CD8$^+$ T cells, that reportedly play an important role in antitumor activity in cancer immunotherapy [25, 26], harboring CCR4 expression accompanied by Treg cell reduction after mogamulizumab administration, indicating the importance of developing more specific Treg cell-targeted therapies.

Results

Mogamulizumab administration is well tolerated, but induces limited clinical efficacy.

Thirty-nine patients with advanced CCR4-negative solid cancer received mogamulizumab at two dosages (0.1 and 1.0 mg/kg) cohorts in this phase Ib study (**Table 1**). Their median age was 65 years, and 11 esophageal cancer, 12 lung cancer, 6 malignant melanoma, 5 gastric cancer and 5 ovarian cancer patients were administered mogamulizumab 2 to 23 times. In the 0.1 mg/kg cohort, a total of 198 adverse events (AEs) and 65 mogamulizumab-related AEs were observed, while a total of 126 AEs and 49 mogamulizumab-related AEs were observed in the 1.0 mg/kg cohort. Among the mogamulizumab-related AEs, skin disorders and lymphopenia were the most frequently observed (**Table 2**).

One PR esophageal cancer patient and 5 SD lung or esophageal cancer patients were confirmed as exhibiting objective clinical responses according to the RECIST criteria. The median PFS and OS were 67 and 271 days in the 0.1 mg/kg cohort and 65 and 272 days in the 1.0 mg/kg cohort, respectively (**Table 1** and **Supplemental Figure 1A**).

CyTOF analyses reveal the comprehensive immunological features after mogamulizumab treatment.

The unexpected observation of limited clinical responses prompted us to investigate the comprehensive immunological features after mogamulizumab treatment [24]. We subjected pre- (within two weeks before treatment) and post-treatment PBMC (peripheral blood mononuclear cell) samples from patients, from whom sufficient amounts of samples were available to CyTOF analyses (**Figure 1A**). Comprehensive immunological analyses with CyTOF showed a decrease in CCR4-positive cells after mogamulizumab administration irrespective of the mogamulizumab dosage (0.1 and 1.0 mg/kg). In particular, mogamulizumab significantly reduced some subpopulations of $CD4^+$ T cells such as Treg cells, although most $CD4^+$ T cell populations were increased, which was in line with our previous reports (**Figure 1B** and **1C**) [24]. Unexpectedly, while most $CD8^+$ T cell populations were increased, a subpopulation of $CD8^+$ T cells was decreased by mogamulizumab treatment (**Figure 1C**). Unbiased clustering with CYBERTRACK further revealed a marked reduction in several finely clustered cell populations, such as cluster 10 (containing Treg cells) and cluster 12 (containing $CD8^+$ T cells), whereas activated non-Treg $CD4^+$ T cells expressing PD-1 (cluster 16) were increased (**Figure 1D-1G** and **Supplementary Figure 2**). Other immune cells, such as B cells and monocytes, were not significantly changed after mogamulizumab administration (**Figure 1B**, **1D, 1E** and **Supplementary Figure 2**). These data suggest that mogamulizumab effectively depletes Treg cells as expected, but a subpopulation of $CD8^+$ T cells may also be influenced.

Mogamulizumab treatment efficiently depletes Treg cells.

To confirm these findings, we examined additional PBMCs with flow cytometry. Total $CD4^+$ T cells were significantly decreased while $CD8^+$ T cells were increased after mogamulizumab administration, reflecting the previous data showing the CCR4 expression pattern (**Figure 2A** and **2B**) [24]. To further explore the populations influenced by mogamulizumab, we divided $CD4^+$ T cells into five fractions as previously reported [9, 13, 22]. CCR4 expression was mainly detected in Fr. II eTreg cells and also in Fr. III non-Treg cells

with low FoxP3 expression (**Figure 2C**) [13, 23]. These CCR4-expressing Fr. II eTreg cells and Fr. III non-Treg cells were significantly decreased, while some $CD4^+$ T cell populations particularly naive $CD45RA^+CD4^+$ T cells were, although not significant, increased after mogamulizumab administration (**Figure 2C-2E**). In addition, the frequency of Fr. I naive Treg cell population was also prone to increase (**Figure 2C** and **2D**). From some patients with a long follow-up, we could sequentially collect PBMC samples. Most patients, except for one patient whose Treg cells lost the expression of CCR4, showed a long-lasting reduction in eTreg cells during mogamulizumab administration (**Figure 2F**). Furthermore, we were able to collect tumor tissues pre- and post- mogamulizumab treatment from a gastric cancer patient. eTreg cells were markedly decreased after mogamulizumab administration (**Figure 2G**). Therefore, mogamulizumab, regardless of the dosage tested (0.1 and 1.0 mg/kg), effectively depletes eTreg cells in peripheral blood and probably in tumors, although the loss of CCR4 expression may hamper the effect.

Central-memory $CD8^+$ T cells are reduced by mogamulizumab treatment.

Based on the possible reduction in the subpopulation(s) of $CD8^+$ T cells according to the CyTOF analyses (Figure 1), we extensively explored the changes in detailed $CD8^+$ T cell populations. Central-memory $CD8^+$ T cells were significantly reduced after mogamulizumab administration, although $CD8^+$ T cells as a whole were significantly increased (Figure 2B, 3A and 3B). In addition, effector-memory $CD8^+$ T cells and terminally-differentiated effector-memory (TEMRA) $CD8^+$ T cells showed a trend, although not significant, toward increase after mogamulizumab treatment (Figure 3A and 3B) [27]. In accordance with this, central-memory $CD8^+$ T cells, but not effector-memory $CD8^+$ T cells or TEMRA $CD8^+$ T cells expressed CCR4, although the level of CCR4 expression was significantly lower than that of eTreg cells (Figure 3C and 3D). The different expression levels were attributed to an increase in chromatin accessibility in eTreg cells compared to that in central-memory $CD8^+$ T cells, as detected by the ATAC-seq peaks (Figure 3E). Moreover, an open chromatin region which was only detected by Treg cells was compatible with the binding site of FoxP3 (Figure 3E), which is the master transcription factor of Treg cells [8, 9], indicating the enhancement of CCR4 expression in Treg cells under FoxP3 control.

We then interrogated the distinct impacts of mogamulizumab on central-memory $CD8^+$ T cells in relation to clinical responses, given the important role of central-memory $CD8^+$ T cells in antitumor immunity [25, 26]. To address the potential for mogamulizumab binding, the ratio of CCR4 expression in central-memory $CD8^+$ T cells to that in eTreg cells was analyzed, and relatively decreased CCR4 expression in central-memory $CD8^+$ T cells compared to that in eTreg cells was observed in long-term survivors ($\geq$1 year) than in short-term survivors (<1 year) (Figure 3F). Accordingly, the reduction in central-memory $CD8^+$ T cells was subsided in long-term survivors compared to short-term survivors (Figure 3G). Thus, central-memory $CD8^+$ T cells that express CCR4 are concomitantly reduced along with eTreg cells by mogamulizumab treatment (0.1 and 1.0 mg/kg), particularly in short-term survivors.

NK cells show an exhausted phenotype in long survivors.

Due to the uncoupling of clinical efficacy and CCR4 expression in eTreg cells and central-memory $CD8^+$ T cells, we further explored the potential involvement of NK cell function in the clinical efficacy of mogamulizumab because mogamulizumab possesses enhanced antibody-dependent cellular cytotoxicity (ADCC) activity via a defucosylated Fc region [28]. NK cells exhibited an exhausted phenotype, which was determined by the expression of PD-1 and LAG-3, in some patients particularly in long-term survivors (Figure 4A and 4B), indicating the presence of impaired ADCC activity in long-term survivors [29]. Patients, from whom the data regarding both CCR4 expression and NK cell exhaustion were available, were divided into long-term survivors and short-term survivors, and CCR4 expression and NK cell exhaustion were compared. Long-term survivors harbored lower expression of CCR4 in central-memory $CD8^+$ T cells and higher levels of NK cell exhaustion (Figure 4C).

Central-memory $CD8^+$ T cells and eTreg cells exhibit a different sensitivity to mogamulizumab treatment.

To gain a mechanistic insight into the *in vivo* data, PBMCs from healthy individuals were cultured with the titrated concentrations (10 - 0.001 mg/ mL) of mogamulizumab reflecting the *in vivo* dosages based on the pharmacokinetics data from previous clinical trials [24, 28, 30]. Both eTreg cells and central-memory $CD8^+$ T cells were significantly reduced after adding mogamulizumab with 10 mg/ mL, which reflected the dosage of 1.0 mg/kg *in vivo*. However, less than 0.1 mg/ mL (less than 0.01 mg/kg *in vivo*) mogamulizumab selectively depleted eTreg cells compared with central-memory $CD8^+$ T cells, indicating that eTreg cells are preferentially targeted by mogamulizumab due to their higher CCR4 expression compared to that of central-memory $CD8^+$ T cells (Figure 4D and 4E). Altogether, the low clinical efficacy of mogamulizumab in solid cancer patients is partially attributed to the unexpected decrease in central-memory $CD8^+$ T cells with CCR4 expression accompanied by Treg cell reduction, considering the relatively favorable clinical courses in patients who had central-memory $CD8^+$ T cells with lower CCR4 expression compared with eTreg cells and/or in whom NK cells exhibited an exhausted phenotype, which avoided the unexpected depletion of antitumor effector components.

Discussion

Treg cell-targeted therapies have been tested in the clinic with high expectations. Despite of the promising preclinical studies [10, 11, 12, 13, 31], no Treg cell-targeted therapy has been successfully applied in the clinic. The poor clinical outcome was thought to be attributed to the low specificity of the reagents used for Treg cell deletion [13]. In this study, we employed anti-CCR4 mAb (mogamulizumab) because CCR4 is selectively expressed by eTreg cells, which comprise a major population of tumor-infiltrating Treg cells, but not by other effector T cells, including Th1 type $CD4^+$ T cells and $CD8^+$ T cells, which are reportedly critical for antitumor immunity [23, 25, 26, 32]. While mogamulizumab efficiently depleted eTreg cells in peripheral blood, most patients who were treated with mogamulizumab did not exhibit tumor regression, as observed in our previous phase 1a study [24]. Our comprehensive immune-monitoring assays revealed that central-memory $CD8^+$ T cells with CCR4 expression were concomitantly reduced along with Treg cells after mogamulizumab administration. Given the importance of T cell clonal replacement rather than the

reinvigoration of pre-existing activated T cells after ICB and the genetic transfection into non-activated (relatively naive) $CD8^+$ T cells instead of effector cells in adoptive T cell therapies [25, 26], mogamulizumab may concurrently deplete harmful Treg cells and beneficial central-memory $CD8^+$ T cells that must be evoked and activated upon Treg cell depletion, cancelling antitumor clinical efficacy.

Mogamulizumab was approved for the treatment of CCR4-positive adult T-cell leukemia/lymphoma (ATLL) caused by human T-lymphotropic virus type 1 (HTLV-1) and peripheral T-cell lymphoma (PTCL) in Japan in 2012 [28, 33], and has also been tested in another HTLV-1-associated disease, HTLV-1-associated myelopathy-tropical spastic paraparesis (HAM-TSP) [30]. Additionally, the FDA and EMA approved mogamulizumab as a treatment for patients with 2 subtypes of cutaneous T-cell lymphoma (CTCL: mycosis fungoides and Sézary syndrome) who have received at least 1 prior systemic therapy in 2018 [34]. In dose-escalation studies for the treatment of ATLL and HAM-TSP, lower dosages (0.003 - 0.03 mg/kg) of mogamulizumab were examined, and a significant reduction of Treg cells in peripheral blood was observed, as was observed in this study [24, 28, 30]. In the treatment of CCR4-positive ATLL, PTCL and CTCL, mogamulizumab works as a “molecular-targeted reagent” that directly kills malignant cells via ADCC. The target cells (CCR4-positive cells) of mogamulizumab must be abundant in the host during the treatment of CCR4-positive ATLL, PTCL and CTCL compared to those in the current study, in which mogamulizumab was used as a “cancer immunotherapy reagent” that kills eTreg cells in advanced or recurrent solid (CCR4-negative) tumor patients. One can envision that excessive doses of mogamulizumab targeted central-memory $CD8^+$ T cells with CCR4 expression, though these cells showed much lower expression of CCR4 than eTreg cells due to the difference in the epigenetic status; a low dosage of mogamulizumab, such as 0.01 mg/kg - 0.001 mg/kg, at which Treg cell reduction in peripheral blood was observed [30], may be sufficient and optimal for Treg cell depletion to avoid the concomitant reduction of central-memory $CD8^+$ T cells. Indeed, our *in vitro* experiments showed the relatively selective depletion of Treg cells at lower concentrations. In addition, patients who experienced clinical benefits exhibited a smaller reduction of central-memory $CD8^+$ T cells: in these patients, central-memory $CD8^+$ T cells harbored lower CCR4 expression and/or NK cells exhibited an exhausted phenotype, strongly suggesting the avoidance of mogamulizumab-mediated ADCC. Moreover, in a phase 1 dose-escalation study in ATLL patients, durable clinical responses, which are often observed in response to cancer immunotherapy were reportedly observed at lower dosages (0.01 mg/kg) than the dosages (0.1 and 1.0 mg/kg) used in the clinic and in our current study [28].

The maximum tolerated dose, which is the highest dose of a drug that does not cause unacceptable side effects, is generally employed as the optimal dose for cytotoxic anticancer reagents. In cancer immunotherapy, the maximum tolerated dose may not always be the optimal dose. When mogamulizumab is used for Treg cell depletion as a “cancer immunotherapy reagent”, doses lower than the maximum tolerated dose could provide favorable clinical outcomes. However, as the patient samples tested in our study were limited, the performance of wide range of dose-escalation studies considering durable clinical responses and dose-de-escalation studies with comprehensive immunological analyses is warranted.

Another plausible explanation for the impairment of clinical responses to mogamulizumab in advanced or recurrent solid (CCR4-negative) tumor patients is that mogamulizumab did not sufficiently deplete eTreg cells in the TME. Recent studies addressing comprehensive gene expression profiling in tumor-infiltrating Treg cells in colorectal cancer, non-small cell lung cancer and breast cancer have revealed that CCR4 is not the optimal molecule for targeting tumor-infiltrating Treg cells, since CCR4 is predominantly expressed by eTreg cells in peripheral blood rather than those in the TME [35, 36]. We have previously shown that CCR4 is highly expressed by tumor-infiltrating Treg cells in melanoma patients [23]. As CCR4 acts as a skin-homing chemokine receptor, tumor-infiltrating Treg cells collected from skin lesions of melanoma may show higher expression of CCR4 compared to those in other tissues [32]. In addition, NK cell activity is crucial for ADCC medicated by mogamulizumab, which harbors enhanced ADCC activity via its defucosylated Fc region and is often impaired in the TME. Nevertheless, we observed a marked decrease in eTreg cells in the TME in a gastric cancer patient. Therefore, studies with a large number of patients are warranted.

An original animal study showing the potential application of Treg cell-targeted cancer immunotherapy implicates the limited window for Treg cell-targeted therapy; Treg cell depletion induces tumor regression in some tumor lines, such as Meth A and RL-male 1, but not in others, such as AKSL2 and RL-female8 [14]. Thus, we need to identify the biomarker(s) that can identify the tumors in which Treg cells are essential for survival and growth through clarifying the immune suppressive network controlled by Treg cells, as has been done for ICB therapies [5, 6]. Our previous study has illustrated the potential application of Treg cell-targeted therapy in high-risk patients for hyperprogressive diseases upon PD-1 blockade therapy [37].

In conclusion, the low clinical efficacy of monotherapy with mogamulizumab in solid cancer patients is at least partly attributed to the unexpected decrease in central-memory $CD8^+$ T cells with CCR4 expression accompanied by Treg cell reduction due to the use of excessive doses of mogamulizumab. We therefore need to carefully determine the optimal dose of mogamulizumab for cancer immunotherapy. The efficient depletion of tumor-infiltrating eTreg cells in a gastric cancer patient encourages us to examine mogamulizumab as a Treg cell depletion reagent in further studies with large cohorts for clinical application.

Methods

Patients

Patients over 20 years old with advanced or recurrent CCR4-negative cancer were enrolled in this study from October 2013 to April 2015. CCR4 expression was determined by immunohistochemistry with anti-CCR4 mAb as described in **Immunohistochemistry**. Eligibility criteria included a good performance status (an Eastern Cooperative Oncology Group performance status of 0 to 2) and the following laboratory values: absolute neutrophil count ≥ 1,500/μL, hemoglobin ≥ 8.0 g/dL, platelet count ≥ 75,000/μL, total bilirubin ≤ 2.0 mg/dL, AST ≤ 2.5 × the upper limit of the normal range (UNL), ALT ≤ 2.5 × UNL, serum creatinine ≤ 1.5 mg/dL, and arterial blood oxygen saturation ≥ 93%. All patients underwent electrocardiography to confirm the absence of cardiac abnormalities requiring therapeutic intervention and

that the left ventricular ejection fraction was at least 50%. Patients were excluded if they had an active infection, a history of organ transplantation, active concurrent cancer, any autoimmune diseases, central nervous system involvement, hepatitis B or C virus infection, HIV infection or previous ICB therapy.

Study design

This multi-institutional, open-label, two-arm, phase Ib study is a part of an investigator-initiated phase Ia/Ib clinical trial of mogamulizumab administration in patients with CCR4-negative advanced or recurrent solid tumors (NCT01929486). The primary objectives were to characterize the safety and the effect of Treg cell depletion in peripheral blood. The secondary objectives were to assess the antitumor activity and to determine the recommended phase II dose. Twenty and nineteen patients were randomly enrolled in cohorts treated with dosages of 1.0 and 0.1 mg/kg mogamulizumab, respectively, and received the drug weekly for 8 weeks, which was followed by monthly intravenous infusion until disease progression was observed. These two dosages of mogamulizumab were determined as the maximum-tolerated dose and minimal dose in our previous phase Ia study [24].

Toxicity was graded according to the National Cancer Institute Common Terminology Criteria for Adverse Events (version 4.0). Clinical responses were evaluated at 12 weeks after the first mogamulizumab administration or at the point of study discontinuation using computed tomography scans. The effects were determined according to the RECIST criteria (version 1.1). Progression-free survival (PFS) was defined from the day of the first mogamulizumab administration until the day of progressive disease (PD) detection. Peripheral blood samples were serially collected, and PBMCs were isolated by density gradient centrifugation with Ficoll-Paque (GE Healthcare, Little Chalfont, UK). To collect TILs, fresh tumor tissues were minced and treated with a gentleMACS Dissociator (Miltenyi Biotec, Bergisch Gladbach, Germany) as previously described [37, 38], and the prepared cells were subjected to immune-monitoring assays.

The protocol was approved by the institutional review boards at each participating site, and all patients provided written informed consent before enrollment in accordance with the Declaration of Helsinki.

Immunohistochemistry

Biopsy samples were formalin-fixed, paraffin-embedded, and sectioned before they were placed onto slides for immunohistochemistry, which was conducted with anti-CCR4 mAb (KM2160; Kyowa Hakko Kirin) as previously reported [24]. CCR4 positivity was evaluated by the review committee with central evaluation.

CyTOF analyses

CyTOF staining and analysis were performed as described [39]. The antibodies used in the CyTOF analyses are summarized in **Supplementary Table 1**. Cells were subjected to staining after washing with PBS supplemented with 2% fetal calf serum (FCS, Biosera, Orange, CA, USA) (washing solution). The cells were incubated in 5 μM of Cell-ID rhodium solution (Fluidigm, South San Francisco, CA) in PBS, washed using washing solution, and stained with a mixture of surface-staining antibodies. After washing, the cells were fixed and permeabilized using a Foxp3/Transcription Factor Staining Buffer Set (Thermo Fisher Scientific,

Waltham, MA) according to the manufacturer's instructions. The fixed and permeabilized cells were stained with the intracellular antibodies. After washing twice, the cells were allowed to rest overnight in 125 nM MaxPar Intercalator-Ir (Fluidigm) diluted in PBS solution with 2% paraformaldehyde at 4°C. The cells were then washed once with washing solution and twice with MaxPar water (Fluidigm) and distilled water with minimal heavy element contamination to reduce the background level. The cells were resuspended in MaxPar water supplemented with 10% EQ Four Element Calibration Beads (Fluidigm) and then were applied to the Helios instrument (Fluidigm), and data were acquired at a speed below 300 events/second.

Preprocessing and analysis of CyTOF data

The data from the pre- and post-mogamulizumab administration samples were combined for each patient, and batch effects were removed using ResNet [40]. After removing the batch effects, the data were combined, and the UMAP projections were generated using the R package "umap". A modified version of CYBERTRACK was used for clustering the CyTOF data [41]. The cluster sizes were determined by the Elbow method, and debris clusters were removed for further analyses.

Flow cytometry analyses

Flow cytometry staining and analyses were performed as described [23, 39, 42]. The antibodies used in the flow cytometry analyses are summarized in **Supplementary Table 2**. Cells (PBMCs and TILs) were washed using washing solution and subjected to staining with surface antibodies. Intracellular staining of FoxP3 was performed with anti-FoxP3 mAb and Foxp3/Transcription Factor Staining Buffer Set (Thermo Fisher Scientific) according to the manufacturer's instructions. After washing, the cells were analyzed with an LSRFortessa instrument (BD Biosciences, San Jose, CA) and FlowJo software (Treestar, Ashland, OR). The dilution of the staining antibodies was performed according to the manufacturer's instructions.

ATAC-seq data processing

ATAC-seq data reported by Calderon et. al [43] were employed{Calderon, 2019 #1}. Law FASTQ files about naive $CD8^+$ T cells, central-memory $CD8^+$ T cells, effector-memory $CD8^+$ T cells and Treg cells were downloaded from the Gene Expression Omnibus (accession no. GSE118189). Trim-Galore (https://www.bioinformatics.babraham.ac.uk/projects/trim_ galore/) was utilized for trimming adaptor sequence and filtering low quality reads. The filtered FASTQ files were aligned to GRCh38 genome using Bowtie2 v2.4.1 [44]. The reads mapped to chrM, mapping quality < 30 and with the flags "- F 1804" and "-f 2" were filtered out using samtools v1.9 (http://www.htslib.org), and the duplicated reads were also removed using Picard Tools v1.119 (https://broadinstitute.github.io/picard/). Then, the resultant BAM files for each cell type were merged. Chromatin accessibility signals were calculated form merged BAM files using deepTools2 [45]. For normalizing signals, we used reads counts data mapped to ATAC peaks regions detected by MACS2 [46] under the parameters "-nonodel -nolamda -keep-dup all -call summits". The MACS2 narrow peak files from each cell type were merged using bedtools2 (https://bedtools.readthedocs.io/en/latest/). The mapped reads in merged peaks region were counted

using featureCounts [47]. The size factors were calculated using R “DESeq” package, and then ATAC signals were normalized. For visualizing ATAC signals, Integrative Genomics Viewer was used [48].

ChIP-seq data processing

FOXP3 ChIP-seq data reported by Birzele et. al. and Schmldl et. al. were employed [49, 50]. Law FASTQ files about Treg cells and naive Treg cells were downloaded from the NCBI SRA (SRP006674) and GEO (GSE43119), respectively. Trim-Galore was used for trimming adaptor sequence and filtering low quality reads. We then aligned filtered FASTQ files to GRCh38 genome using Bowtie2 v2.4.1 [44]. The duplicated reads and reads having mapping quality < 4 were filtered out using Picard Tools v1.119 and samtools v1.9, respectively. The resultant BAM files for each cell type were merged. FOXP3 ChIP signals were calculated from merged BAM files using deepTools2 under the parameters “-bs=10 –normalize Using CPM –extendReads 200” [45]. For visualizing FOXP3 ChIP-seq signals, Integrative Genomics Viewer was used [48].

T cell culture

PBMCs from healthy individuals were cultured with in a round-bottom 96-well plate with medium containing IL-2 (30 U/mL). The indicated dose of mogamulizumab was added to some wells during the entire culture period. After 7 days, the cells were subjected to a BD FACSymphony A3 instrument (BD Biosciences) and FlowJo software (Treestar).

Statistical analysis

The relationships between groups were compared using a t-test or the nonparametric Mann-Whitney U test. For multiple group comparisons, the Bonferroni method was employed. PFS and OS were defined as the time from the initial mogamulizumab administration until the first observation of disease progression and death from any cause, respectively. PFS and OS were investigated with the Kaplan–Meier method and were compared among the groups using the log-rank test or Cox regression proportional hazards analysis. Statistical analysis was performed with GraphPad Prism8 (GraphPad Software, San Diego, CA) or R version 3.1.1 (R Foundation for Statistical Computing, Vienna, Austria). *P* values less than 0.05 were considered significant.

Declarations

In Memoriam: This article is dedicated to the memory of the late Dr. E. Nakayama.

Acknowledgments: We are grateful to Drs. Y. Ueda, H. Nagase, K. Kurose, Y. Ohue, T. Oguri, A. Arakawa, M. Nakamura, Y. Mori, T. Ishida, H. Matsushita, M. Anraku, Y. Seto, M. Sugaya for their clinical support. We thank Ms. H. Danbee, Y. Tada, T. Takaku, M. Nakai, T. Sugaya, Y. Ishige and E. Tanji for their technical assistance.

This study was supported by Grants-in-Aid for Scientific Research (S) grant no. 17H06162 (H.N.), for Challenging Exploratory Research grant no. 16K15551 (H.N.), for Research Activity Start-up grant no.

15H06878 (Y.M.), for Young Scientists (B) grant no. 17K15738 (Y.M.) and for Scientific Research (B) grant no. 19H03729 (H.W.) from the Ministry of Education, Culture, Sports, Science and Technology of Japan; by the Projects for Cancer Research by Therapeutic Evolution [P-CREATE, no. 16cm0106301h0001 (H.N.) and no. 17cm0106322h0002 (Y.M.)] and by the Development of Technology for Patient Stratification Biomarker Discovery grant [no.19ae0101074s0401 (R.U. and H.N.)] from the Japan Agency for Medical Research and Development (AMED) and by the National Cancer Center Research and Development Fund [no. 28-A-7 and 31-A-7 (H.N.)].

Author contributions: Y.M. and H.W. equally contributed to this work.

Y.M, D.S., T.I., K.M., T. Shimamura., E.N. and H.N. performed the experiments and analyzed the data. H.W., T. Saito., S.S., T.K., K.K, J.N., T.F., S.I., M.O., T.D., Y.D. and R.U. collected clinical specimens and performed analyses of clinical data. Y.M, H.W., E.N., R.U. and H.N. conceived the project. Y.M, H.W., T. Saito., R.U. and H.N. wrote the paper.

Competing interests: H.W. received research funding from Ono Pharmaceutical and Kyowa Kirin, and honoraria from Ono Pharmaceutical, Chugai Pharmaceutical, MSD and Bristol-Myers Squibb outside of this study. Department of Clinical Research in Tumor Immunology, Osaka University Graduate School of Medicine is a joint research laboratory with Shionogi & Co., Ltd. K.T. received honoraria and research funding from Ono Pharmaceutical, MSD, Shionogi, Bristol-Myers Squibb, Chugai Pharmaceutical, Amgen, Astellas Pharmaceutical, Oncolys BioPharma, Parexel and Merck Serono outside of this study. K.K. received research funding from TAKARA BIO and MSD outside of this study. Department of Immunotherapeutics, The University of Tokyo Hospital is endowed by TAKARA BIO. T.F. received research funding from Ono Pharmaceutical outside of this study. S.I. received honoraria and research funding from Ono Pharmaceutical, Takeda, Sanofi, Bristol-Myers Squibb, Janssen, Celgene and Daichi-Sankyo, and research funding from Kyowa Kirin, Abbvie, Chugai Pharmaceutical, MSD and Gilead outside of this study. M.O. received research funding from Thyas, Sysmex and Pole Star outside of this study. T.D. received honoraria and research funding from Lilly, Kyowa Kirin, MSD, Daiichi-Sankyo, Sumitomo Dainippon Pharma, Taiho Pharmaceutical, Novartis, Boehringer Ingelheim, Chugai Pharmaceutical, Bristol-Myers Squibb, Abbvie, and research funding from Merck Serono, Janssen Pharma, Pfizer, Quintiles, Eisai, and honoraria from Amgen, Takeda, Bayer, Rakuten Medical, Ono Pharmaceutical, Astellas Pharmaceutical, Oncolys BioPharma outside of this study. Y.D. received honoraria and research funding from Ono Pharmaceutical, Taiho Pharmaceutical, and research funding from Chugai Pharmaceutical, Covidien Japan, Jhonson & Jhonson and honoraria from Otsuka Pharmaceutical outside of this study. R.U. received research funding from Ono Pharmaceutical, Chugai Pharmaceutical and Kyowa Kirin outside of this study. H.N. received honoraria and research funding from Ono Pharmaceutical, Chugai Pharmaceutical, MSD and Bristol-Myers Squibb, and research funding from Taiho Pharmaceutical, Daiichi-Sankyo, Kyowa Kirin, Zenyaku Kogyo, Oncolys BioPharma, Debiopharma, Asahi-Kasei, Sysmex, Fujifilm, SRL, Astellas Pharmaceutical, Sumitomo Dainippon Pharma and BD Japan outside of this study. All other authors declare no competing financial interests.

References

1. Hanahan D, Weinberg RA. Hallmarks of cancer: the next generation. *Cell* **144**, 646–674 (2011).
2. Borghaei H, *et al.* Nivolumab versus Docetaxel in Advanced Nonsquamous Non-Small-Cell Lung Cancer. *N Engl J Med* **373**, 1627–1639 (2015).
3. Rizvi NA, *et al.* Cancer immunology. Mutational landscape determines sensitivity to PD-1 blockade in non-small cell lung cancer. *Science* **348**, 124–128 (2015).
4. Schreiber RD, Old LJ, Smyth MJ. Cancer immunoediting: integrating immunity's roles in cancer suppression and promotion. *Science* **331**, 1565–1570 (2011).
5. Sharma P, Allison JP. Immune checkpoint targeting in cancer therapy: toward combination strategies with curative potential. *Cell* **161**, 205–214 (2015).
6. Sharma P, Hu-Lieskovan S, Wargo JA, Ribas A. Primary, Adaptive, and Acquired Resistance to Cancer Immunotherapy. *Cell* **168**, 707–723 (2017).
7. Sakaguchi S, Sakaguchi N, Asano M, Itoh M, Toda M. Immunologic self-tolerance maintained by activated T cells expressing IL-2 receptor a-chains (CD25). Breakdown of a single mechanism of self-tolerance causes various autoimmune diseases. *J Immunol* **155**, 1151–1164 (1995).
8. Sakaguchi S. Naturally arising Foxp3-expressing $CD25^+$ $CD4^+$ regulatory T cells in immunological tolerance to self and non-self. *Nat Immunol* **6**, 345–352 (2005).
9. Sakaguchi S, Miyara M, Costantino CM, Hafler DA. $FOXP3^+$ regulatory T cells in the human immune system. *Nat Rev Immunol* **10**, 490–500 (2010).
10. Curiel TJ, *et al.* Specific recruitment of regulatory T cells in ovarian carcinoma fosters immune privilege and predicts reduced survival. *Nat Med* **10**, 942–949 (2004).
11. Sato E, *et al.* Intraepithelial $CD8^+$ tumor-infiltrating lymphocytes and a high $CD8^+$/regulatory T cell ratio are associated with favorable prognosis in ovarian cancer. *Proc Natl Acad Sci U S A* **102**, 18538–18543 (2005).
12. Zou W. Regulatory T cells, tumour immunity and immunotherapy. *Nat Rev Immunol* **6**, 295–307 (2006).
13. Togashi Y, Shitara K, Nishikawa H. Regulatory T cells in cancer immunosuppression - implications for anticancer therapy. *Nat Rev Clin Oncol* **16**, 356–371 (2019).
14. Onizuka S, Tawara I, Shimizu J, Sakaguchi S, Fujita T, Nakayama E. Tumor rejection by in vivo administration of anti-CD25 (interleukin-2 receptor a) monoclonal antibody. *Cancer Res* **59**, 3128–3133 (1999).
15. Shimizu J, Yamazaki S, Sakaguchi S. Induction of tumor immunity by removing $CD25^+CD4^+$ T cells: a common basis between tumor immunity and autoimmunity. *J Immunol* **163**, 5211–5218 (1999).
16. Attia P, Maker AV, Haworth LR, Rogers-Freezer L, Rosenberg SA. Inability of a fusion protein of IL-2 and diphtheria toxin (Denileukin Diftitox, DAB389IL-2, ONTAK) to eliminate regulatory T lymphocytes in patients with melanoma. *J Immunother* **28**, 582–592 (2005).

17. Jacobs JF, *et al.* Dendritic cell vaccination in combination with anti-CD25 monoclonal antibody treatment: a phase I/II study in metastatic melanoma patients. *Clin Cancer Res* **16**, 5067–5078 (2010).
18. Abbas AK, Trotta E, Simeonov DR, Marson A, Bluestone JA. Revisiting IL-2: Biology and therapeutic prospects. *Sci Immunol* **3**, eaat1482 (2018).
19. Walter S, *et al.* Multipeptide immune response to cancer vaccine IMA901 after single-dose cyclophosphamide associates with longer patient survival. *Nat Med* **17**, 1094–1100 (2012).
20. Rini BI, *et al.* IMA901, a multipeptide cancer vaccine, plus sunitinib versus sunitinib alone, as first-line therapy for advanced or metastatic renal cell carcinoma (IMPRINT): a multicentre, open-label, randomised, controlled, phase 3 trial. *Lancet Oncol* **17**, 1599–1611 (2016).
21. Kim JM, Rasmussen JP, Rudensky AY. Regulatory T cells prevent catastrophic autoimmunity throughout the lifespan of mice. *Nat Immunol* **8**, 191–197 (2007).
22. Miyara M, *et al.* Functional Delineation and Differentiation Dynamics of Human $CD4^+$ T Cells Expressing the FoxP3 Transcription Factor. *Immunity* **30**, 899–911 (2009).
23. Sugiyama D, *et al.* Anti-CCR4 mAb selectively depletes effector-type $FoxP3^+CD4^+$ regulatory T cells, evoking antitumor immune responses in humans. *Proc Natl Acad Sci U S A* **110**, 17945–17950 (2013).
24. Kurose K, *et al.* Phase Ia Study of $FoxP3^+$ CD4 Treg Depletion by Infusion of a Humanized Anti-CCR4 Antibody, KW-0761, in Cancer Patients. *Clin Cancer Res* **21**, 4327–4336 (2015).
25. Gattinoni L, Klebanoff CA, Restifo NP. Paths to stemness: building the ultimate antitumour T cell. *Nat Rev Cancer* **12**, 671–684 (2012).
26. Yost KE, *et al.* Clonal replacement of tumor-specific T cells following PD-1 blockade. *Nat Med* **25**, 1251–1259 (2019).
27. Sallusto F, Lenig D, Forster R, Lipp M, Lanzavecchia A. Two subsets of memory T lymphocytes with distinct homing potentials and effector functions. *Nature* **401**, 708–712 (1999).
28. Yamamoto K, *et al.* Phase I study of KW-0761, a defucosylated humanized anti-CCR4 antibody, in relapsed patients with adult T-cell leukemia-lymphoma and peripheral T-cell lymphoma. *J Clin Oncol* **28**, 1591–1598 (2010).
29. Judge SJ, Murphy WJ, Canter RJ. Characterizing the Dysfunctional NK Cell: Assessing the Clinical Relevance of Exhaustion, Anergy, and Senescence. *Front Cell Infect Microbiol* **10**, 49 (2020).
30. Sato T, *et al.* Mogamulizumab (Anti-CCR4) in HTLV-1-Associated Myelopathy. *N Engl J Med* **378**, 529–538 (2018).
31. Nishikawa H, Jager E, Ritter G, Old LJ, Gnjatic S. $CD4^+CD25^+$ regulatory T cells control the induction of antigen-specific $CD4^+$ helper T cell responses in cancer patients. *Blood* **106**, 1008–1011 (2005).
32. Yoshie O, Matsushima K. CCR4 and its ligands: from bench to bedside. *Int Immunol* **27**, 11–20 (2015).
33. Ogura M, *et al.* Multicenter phase II study of mogamulizumab (KW-0761), a defucosylated anti-cc chemokine receptor 4 antibody, in patients with relapsed peripheral T-cell lymphoma and cutaneous T-cell lymphoma. *J Clin Oncol* **32**, 1157–1163 (2014).

34. Kim YH, *et al.* Mogamulizumab versus vorinostat in previously treated cutaneous T-cell lymphoma (MAVORIC): an international, open-label, randomised, controlled phase 3 trial. *Lancet Oncol* **19**, 1192–1204 (2018).
35. De Simone M, *et al.* Transcriptional Landscape of Human Tissue Lymphocytes Unveils Uniqueness of Tumor-Infiltrating T Regulatory Cells. *Immunity* **45**, 1135–1147 (2016).
36. Plitas G, *et al.* Regulatory T Cells Exhibit Distinct Features in Human Breast Cancer. *Immunity* **45**, 1122–1134 (2016).
37. Kamada T, *et al.* PD-1^{+} regulatory T cells amplified by PD-1 blockade promote hyperprogression of cancer. *Proc Natl Acad Sci U S A* **116**, 9999–10008 (2019).
38. Saito T, *et al.* Two FOXP3^{+}CD4^{+} T cell subpopulations distinctly control the prognosis of colorectal cancers. *Nat Med* **22**, 679–684 (2016).
39. Sugiyama E, *et al.* Blockade of EGFR improves responsiveness to PD-1 blockade in EGFR-mutated non-small cell lung cancer. *Sci Immunol* **5**, eaav3937 (2020).
40. Shaham U, *et al.* Removal of batch effects using distribution-matching residual networks. *Bioinformatics* **33**, 2539–2546 (2017).
41. Minoura K, Abe K, Maeda Y, Nishikawa H, Shimamura T. Model-based cell clustering and population tracking for time-series flow cytometry data. *BMC Bioinformatics* **20**, 633 (2019).
42. Maeda Y, *et al.* Detection of self-reactive CD8^{+} T cells with an anergic phenotype in healthy individuals. *Science* **346**, 1536–1540 (2014).
43. Calderon D, *et al.* Landscape of stimulation-responsive chromatin across diverse human immune cells. *Nat Genet* **51**, 1494–1505 (2019).
44. Langmead B, Salzberg SL. Fast gapped-read alignment with Bowtie 2. *Nat Methods* **9**, 357–359 (2012).
45. Ramirez F, *et al.* deepTools2: a next generation web server for deep-sequencing data analysis. *Nucleic Acids Res* **44**, W160-165 (2016).
46. Zhang Y, *et al.* Model-based analysis of ChIP-Seq (MACS). *Genome Biol* **9**, R137 (2008).
47. Liao Y, Smyth GK, Shi W. featureCounts: an efficient general purpose program for assigning sequence reads to genomic features. *Bioinformatics* **30**, 923–930 (2014).
48. Robinson JT, *et al.* Integrative genomics viewer. *Nat Biotechnol* **29**, 24–26 (2011).
49. Birzele F, *et al.* Next-generation insights into regulatory T cells: expression profiling and FoxP3 occupancy in Human. *Nucleic Acids Res* **39**, 7946–7960 (2011).
50. Schmidl C, *et al.* The enhancer and promoter landscape of human regulatory and conventional T-cell subpopulations. *Blood* **123**, e68-78 (2014).

Tables

Table 1. Patient characteristics and clinical responses.

		0.1 mg/kg	1.0 mg/kg	Total
		(n=20)	(n=19)	(n=39)
sex	male/female	12/8	13/6	25/14
age (year-old)	median (range)	66 (47-85)	65 (45-80)	65 (45-85)
BMI (kg/m^2)	mean (sd)	20.6 (3.2)	20.5 (2.7)	20.5 (3.0)
cancer organ				
	esophagus	6	5	11
	lung	6	6	12
	skin	4	2	6
	stomach	2	3	5
	ovary	2	3	5
ECOG	PS; 0/1/2	9/10/1	10/8/1	19/18/2
prior therapies				
	chemotherapy	20	18	38
	surgery	11	14	25
	radiation	8	6	14
	other therapy	3	5	8
total dosage of mogamulizumab				
	median (range)	8 (2-14)	8 (2-23)	8 (2-23)
early escape				
	drop-out	1	0	1
	death	2	2	4
	discontinuation	3	3	6
clinical response				
	PR	0	1	1
	SD	3	2	5
	PD	16	15	31
PFS (days) (RECIST)	median (range)	67 (21-96)	65 (25-491)	66 (21-491)
OS (days)	median (range)	271 (21-	272 (25-	272 (21-

	498)	511)	511)

Table 2 Adverse effects of mogamulizumab administration.

	0.1 mg/kg (n=20)		1.0 mg/kg (n=19)		Total (n=39)	
	cases	events	cases	events	cases	events
AEs	20	198	19	126	39	324
Related AE	19	65	17	49	36	114
Grade 1/2/3/4	16/12/6/1	34/23/7/1	10/14/4/2	23/20/4/2	26/26/10/3	57/43/11/3
decreased lymphocytes	14		11		25	
Grade 1/2/3/4	1/10/2/1		0/7/2/2		1/17/4/3	
dermal disorders	15		11		26	
Grade 1/2/3/4	9/5/1/0		5/6/0/0		14/11/1/0	
Drug eruption, Grade 2			1		1	
Asteatotic eczema, Grade 1	1				1	
Erythema, Grade 1	1				1	
Papule, Grade 2			1		1	
Pruritus, Grade 1	1				1	
Rash, Grade 1/2	1/4		2/3		3/7	
Rash maculo-papular, Grade 1/2/3	5/1/1		3/1/0		8/2/1	

Other Grade 3	increased alanine aminotransferase	decreased appetite
	increased aspartate aminotransferase	hypophosphatasemia
	increased gamma-glutamyl transferase	
	hypophosphatasemia	

Figures

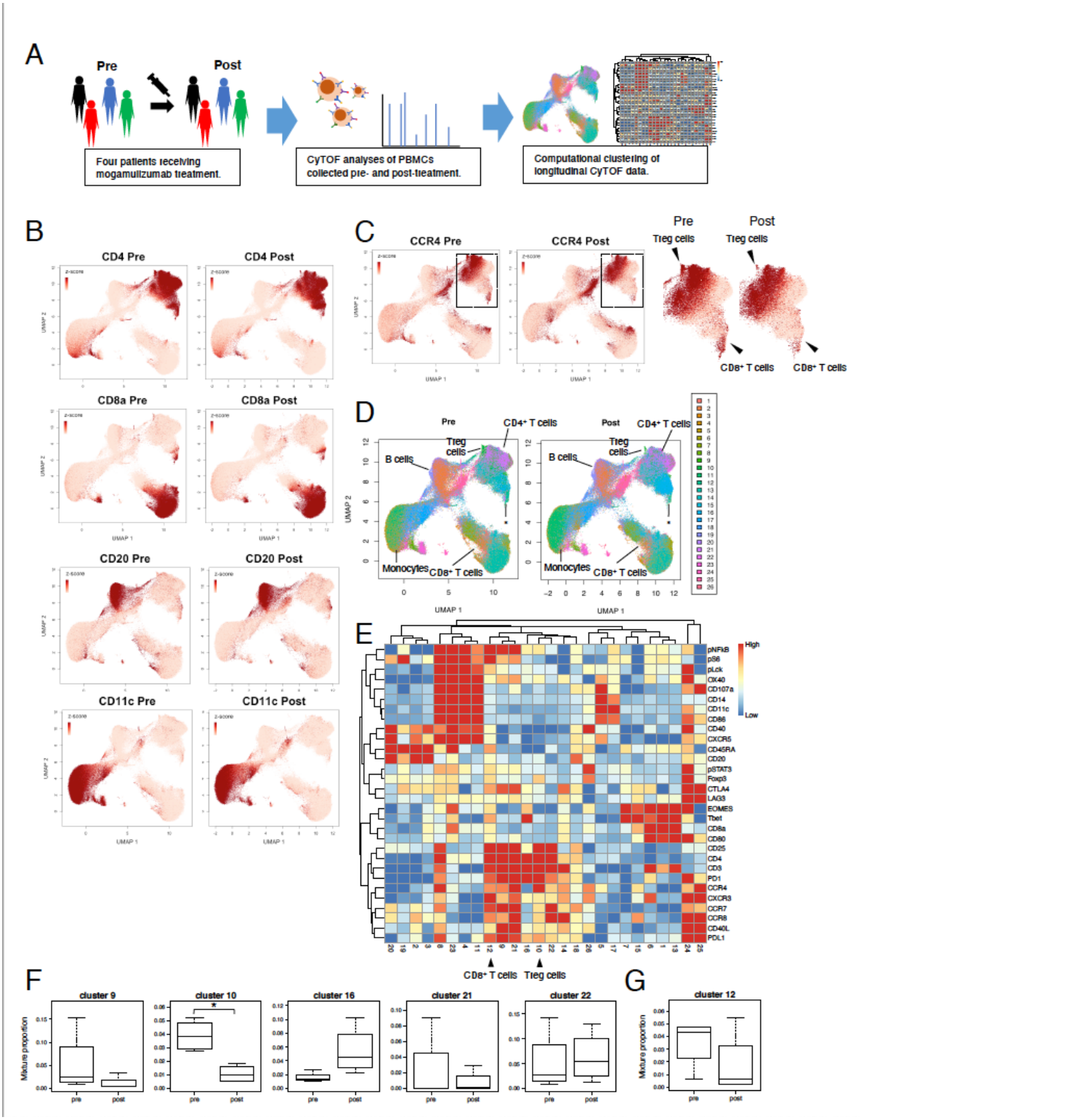

Figure 1

A comprehensive immunological landscape is uncovered by longitudinal CyTOF data obtained from patients treated with mogamulizumab. A. Schematic overview of the CyTOF analyses. PBMCs obtained from pre- and post-mogamulizumab treatment were subjected to CyTOF. B. UMAP projection of cells from pre- and post-mogamulizumab treatment samples is colored according to their scaled expression levels of markers for different cell populations: CD4+ T cells, CD8+ T cells, FoxP3+ T cells, CD20 for B cells, CD11c

for monocytes. C. The UMAP projection is colored according to the scaled expression levels of CCR4. The panels on the right represent the enlarged CD4+ cell populations to clearly show the changes in the expression levels of CCR4 pre- and post-mogamulizumab treatment samples. Black arrowheads represent Treg cells and CD8 T cells. Each dot represents a single cell. Colors were saturated at z-cores 1 and 0 for visualization. D. The UMAP projection is colored according to the cluster assignment by CYBERTRACK2.0. E. Heatmap generated by CYBERTRACK2.0. The rows and columns represent markers and clusters, respectively. Black arrowheads represent Treg cells and CD8+ T cells as in (C). F. Boxplots representing the proportions of CD4+ clusters (clusters 9, 10, 16 and 21) at pre- and post-mogamulizumab treatment. G. Boxplot representing the proportions of cluster 12, which contains CD8+ T cell populations at pre- and post-mogamulizumab treatment. The center line indicates the median, and the box limits indicate the 1st and 3rd quartiles. Whiskers extend to the 1.5x interquartile range. *, $P<0.05$.

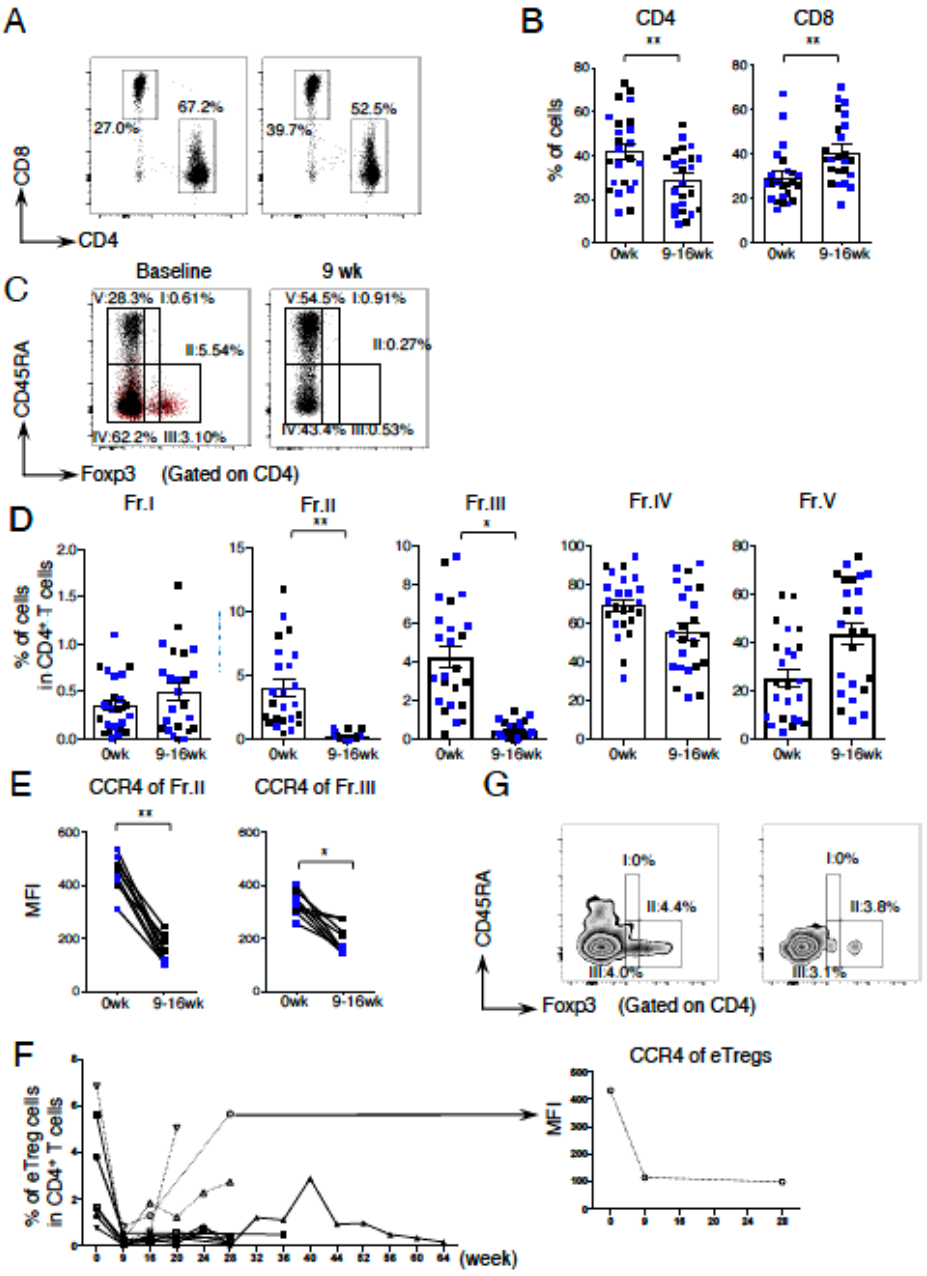

Figure. 2

Figure 2

Mogamulizumab efficiently depletes eTreg cells in both peripheral blood and tumor tissues. A, B. Representative flow cytometry staining for CD4 and CD8 in CD3+ T cells (A) and summary for the frequencies of CD4+ T cells and CD8+ T cells at pre- and post-mogamulizumab treatment (B) are shown. PBMCs obtained from pre- and post-mogamulizumab treatment were subjected to flow cytometry. Pre-treatment samples were collected within two weeks before the initial mogamulizumab administration, and

post-treatment samples were collected at 9-16 weeks after mogamulizumab administration. C, D. Representative flow cytometry staining for CD45RA and FoxP3 in CD4+ T cells (C) and summary for the frequencies of each CD4+ T cell fraction as depicted in (C) at pre- and post-mogamulizumab treatment (D) are shown. PBMC samples as in (A) were subjected to flow cytometry. Red dots, CCR4+ cells; black dots, CCR4- cells. E. Changes in CCR4 expression levels of CCR4+CD4+ T cells (Fr. II and Fr. III) according to the mean fluorescence intensity (MFI) at pre- and post-mogamulizumab treatment are shown. F. Longitudinal changes in the frequencies of Treg cells (Fr. II) in CD4+ T cells at pre- and post-mogamulizumab treatment are shown. G. Fresh tumor samples obtained from gastric cancer patients by endoscopic biopsy at pre- and post-mogamulizumab administration were subjected to flow cytometry. Flow cytometry data for CD45RA and FoxP3 staining in CD4+ T cells are shown. Black dots, patients who received 1.0 mg/kg mogamulizumab; blue dots, patients who received 0.1 mg/kg mogamulizumab. Wk: week, *, $P<0.05$, **, $P<0.01$.

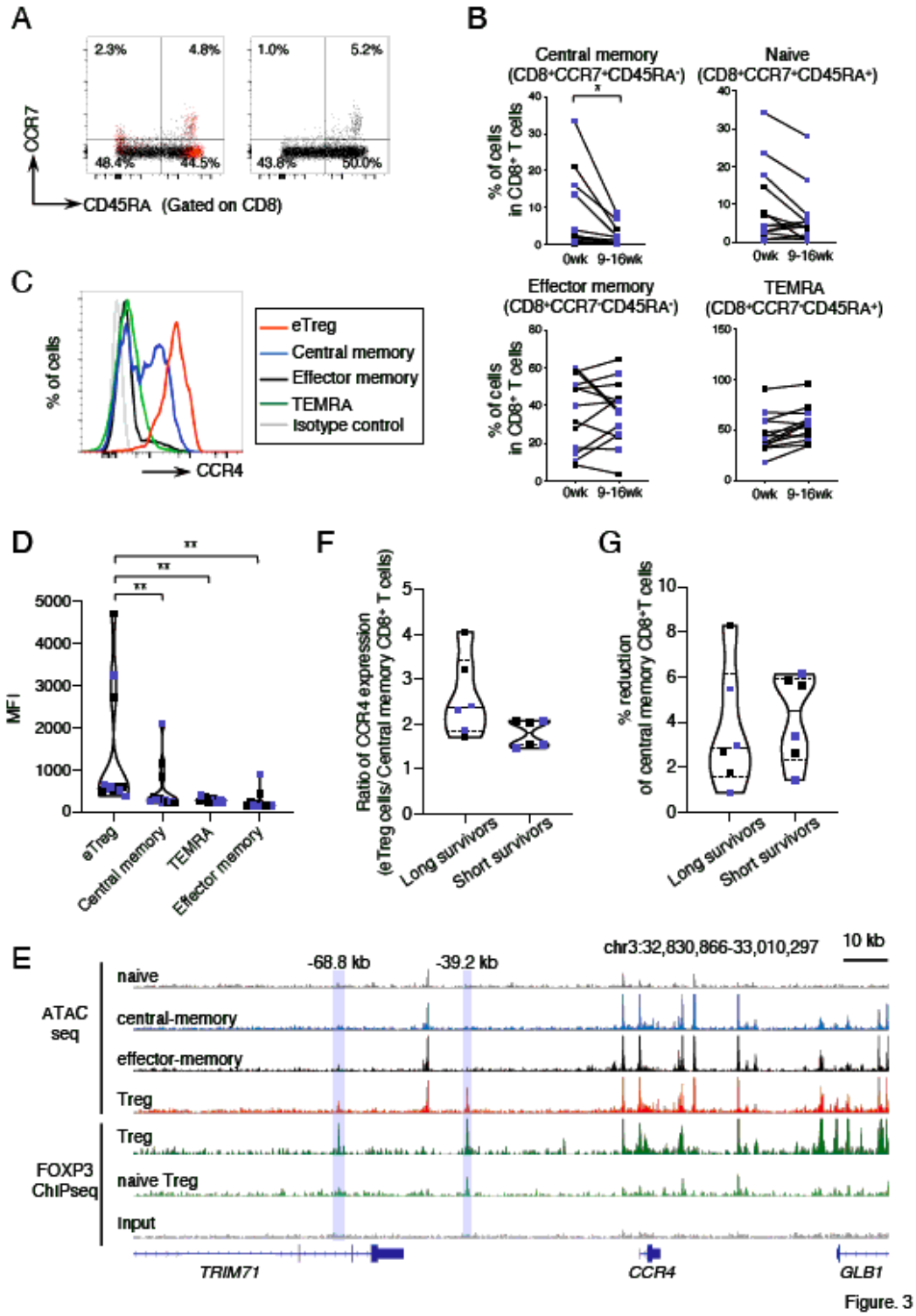

Figure 3

Central-memory CD8+ T cells with CCR4 expression are decreased after mogamulizumab treatment. A, B. Representative flow cytometry staining for CD45RA and CCR7 in CD8+ T cells (A) and summary for the frequencies of each CD8+ T cell fraction as depicted in (A) at pre- and post-mogamulizumab treatment (B) are shown. PBMC samples, as shown in Figure 2, were subjected to flow cytometry. Red dots, CCR4+ cells; black dots, CCR4- cells. C, D. Representative flow cytometry staining for CCR4 in each CD8+ T cell fraction

in comparison with that in eTreg cells (C) and summary for the CCR4 expression levels (MFI) in central-memory CD8+ T cells, effector-memory CD8+ T cells, TEMRA CD8+ T cells and eTreg cells (D) are shown. Red line, eTreg cells; blue line, central-memory CD8+ T cells; black line, effector-memory CD8+ T cells; green line, TEMRA CD8+ T cells; filled gray area, control staining. E. Sequencing tracks of ATAC-seq about four T cell subsets (naive CD8+ T cells, central-memory CD8+ T cells, effector-memory CD8+ T cells and Treg cells) and FOXP3 ChIP-seq about Treg cells around the CCR4 gene locus. The normalized ATAC-seq and ChIP-seq read coverage were used to visualize the tracks. ATAC seq about each T cell subset (gray: naive CD8+ T cells, blue: central-memory CD8+ T cells, black: effector-memory CD8+ T cells, red: Treg cells) and FOXP3 ChIP-seq about Treg cells (green: Treg cells, light green: naive Treg cells, grey: IP control) are shown. F. Ratio of CCR4 expression levels (MFI) in central-memory CD8+ T cells and eTreg cells in long-term survivors (≥1 year) and short-term survivors (< 1 year) is shown. G. % reduction in central-memory CD8+ T cells after mogamulizumab treatment in long-term survivors and short-term survivors is shown. Black dots, patients who received 1.0 mg/kg mogamulizumab; blue dots, patients who received 0.1 mg/kg mogamulizumab. Long-term survivors: Long survivors, short-term survivors: Short survivors. Wk: week, *, $P<0.05$, **, $P<0.01$.

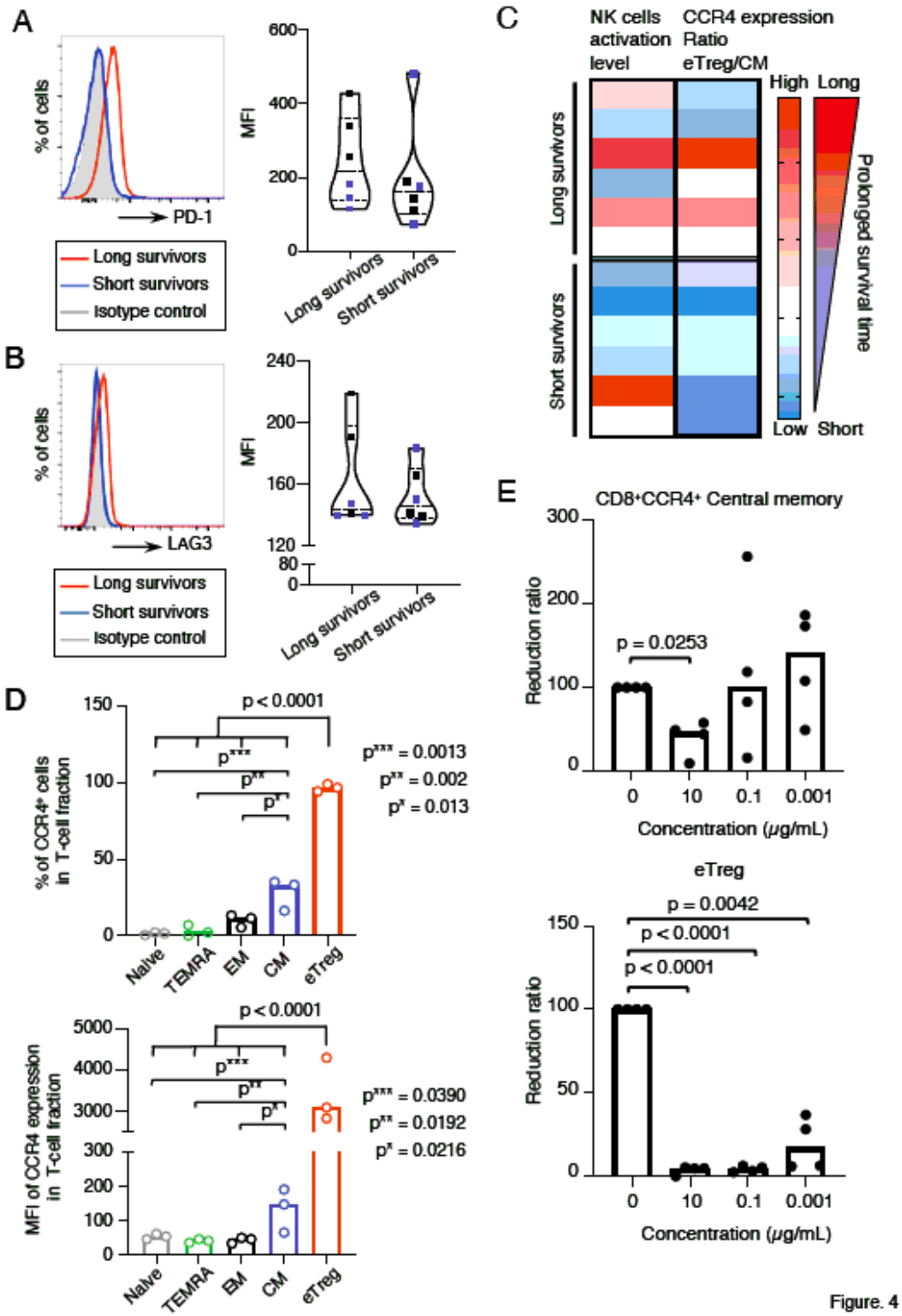

Figure. 4

Figure 4

NK cells exhibit an exhausted phenotype in long-term survivors. A, B. Representative flow cytometry staining for PD-1 (A) and LAG3 (B) in NK cells and summary for the frequencies of NK cells at pre-mogamulizumab treatment in long-term survivors (≥1 year) and short-term survivors (< 1 year) are shown. PBMC samples, as shown in Figure 2, were subjected to flow cytometry. C. Heatmap of the eTreg cell to central-memory CD8+ T cell CCR4 expression ratios (MFI) and the frequency of exhausted NK cells. D. The

frequencies (top) and expression levels (bottom) of CCR4 expression in each CD8+ T cell fraction and eTreg cells in PBMCs from healthy individuals. E. Reduction of central-memory CD8+CCR4+ T cells T cells (top) and eTreg cells (bottom) after mogamulizumab treatment. PBMC samples from healthy individuals (n = 4) were cultured with the indicated dose of mogamulizumab. Changes in each T cell fraction were examined. Black dots, patients who received 1.0 mg/kg mogamulizumab; blue dots patients who received 0.1 mg/kg mogamulizumab. Long-term survivors: Long survivors, short-term survivors: Short survivors. eTreg cells: eTreg, central-memory CD8+ T cells: CM, effector-memory CD8+ T cells: EM, TEMRA CD8+ T cells: TEMRA.

Supplementary Files

This is a list of supplementary files associated with this preprint. Click to download.

- MaedaetalSuppleInformation.pdf